Understanding and simulating mechanochromism in dye-dispersed polymer blends: from atomistic insights to macroscopic properties

Qinfan Wang, Alistar Ottochian, Michele Turelli, Andrea Pucci, Ilaria Ciofini, Carlo Adamo

▶ **To cite this version:**

Qinfan Wang, Alistar Ottochian, Michele Turelli, Andrea Pucci, Ilaria Ciofini, et al.. Understanding and simulating mechanochromism in dye-dispersed polymer blends: from atomistic insights to macroscopic properties. Journal of Molecular Modeling, 2024, 30 (11), pp.387. 10.1007/s00894-024-06174-x . hal-04775536

HAL Id: hal-04775536
https://hal.science/hal-04775536v1

Submitted on 10 Nov 2024

HAL is a multi-disciplinary open access archive for the deposit and dissemination of scientific research documents, whether they are published or not. The documents may come from teaching and research institutions in France or abroad, or from public or private research centers.

L'archive ouverte pluridisciplinaire **HAL**, est destinée au dépôt et à la diffusion de documents scientifiques de niveau recherche, publiés ou non, émanant des établissements d'enseignement et de recherche français ou étrangers, des laboratoires publics ou privés.

Understanding and simulating mechanochromism in dye-dispersed polymer blends: from atomistic insights to macroscopic properties

Qinfan Wang[1], Alistar Ottochian[1], Michele Turelli[1], Andrea Pucci[2], Ilaria Ciofini[1], Carlo Adamo[1*]

[1] *Chimie ParisTech, PSL University, CNRS, Institute of Chemistry for Life and Health Sciences UMR 8060, Theoretical Chemistry and Modeling Team, 75005 Paris, France*
[2] *Dipartimento di Chimica e Chimica Industriale, Università di Pisa, Via Moruzzi 13, 56124 Pisa, Italy*

Abstract

Context

In this work, we propose a computational protocol enabling the simulation of mechanochromic responses in dye-dispersed polymer blends. The main objective is the modeling of the molecular-level structural changes responsible for the modulation of the photophysical properties that lead to the mechanochromic phenomenon. In this demonstrative study we focus on predicting the changes in optical absorption displayed by a model system consisting of a dimer of a tetraphenylethylene derivative dispersed in a polyethylene matrix. The blend is subjected to an external stimulus that causes a modulation of the polymer matrix density that translates, in turn, into the emergence of specific mechanical constraints on the optically active dimers. The accurate description of this phenomenon requires the reliable sampling of the dimer configurations induced by the interaction with the matrix under stress. These molecular geometries are associated with modified electronic structures that confer novel absorption responses to the dispersed dyes.

Methods

In the present contribution, the sampling of these structures is achieved through classical molecular dynamics (MD) simulations including a model element to apply an anisotropic mechanical force. This element allows the microscopic modeling of the chains and dyes structural rearrangements under stress. After the sampling, we compare the results of two approaches for the prediction of the optical response: i) the calculation of a mean response from a statistical average over quantum chemical calculations on the sampled MD structures and ii) a prediction via a more expensive hybrid scheme allowing the relaxation of the sampled molecular geometries in presence of the matrix constraints.

Corresponding Author : carlo.adamo@chimieparistech.psl.eu

1. Introduction

A mechanochromic material is currently understood in a broad sense as any material in solid state that, while experiencing an external mechanical stress, displays a change in color, either in absorption or in luminescence. This definition is based on the observation of a macroscopic effect and actually encompasses very different phenomena occurring at the microscopic scale. These may range from the luminescence of atmospheric N_2 elicited by the interaction with electric fields in the material, generated by charges separated in response to the external stress, as it happens in triboluminescence[1], to dye dispersed into polymer matrices that undergo changes in their optical absorption or emission in response to stimuli applied to the matrix that affect both the interaction between dye units and their intramolecular structure. These dye-polymer blends, in particular, represent an interesting class of functional materials whose tunable optoelectronic properties are becoming increasingly important for several applications, specifically in the domain of sensing technologies[2,3] but with substantial potential to find larger domains of applicability.[4–6]

These behaviours can be better exploited in the final material if both the choice of the dye-polymer pair and the blend manufacturing method through are driven by an understanding of the processes occurring at molecular scale, that are responsible for the macroscopic mechanochromic response.

This understanding is currently missing in large part and multi-scale atomistic modeling represents a natural tool to fill this gap. Even when limiting the discussion to dye-dispersed or doped[7–11] polymer matrices, this goal remains quite ambitious, as the landscape of possible processes is still quite varied. For this class of materials however, it is possible to sketch a general scheme that rests on the idea that mechanochromism originates from the molecular rearrangements experienced by the dispersed chromophores when the matrix is under stress. In the example of a blend under stretch, the macromolecules in the amorphous regions, the ones hosting the chromophores[12,13], respond with a conformational reorganization, *e.g.*, a straightening and alignment along the stimulus direction, this rearrangement affects, in turn, the dispersed dye aggregates either at the supramolecular level, i.e., with a change of the local packing, or at the molecular level with changes in geometry[14].The different degrees at which these effects are displayed depends on the balance between polymer-dye and dye-dye intermolecular interactions and are largely determined by the characteristics of the chosen pair. These changes are naturally reflected in modified optical responses that mirror the reorganization predominantly experienced by the chromophores. For example, when supramolecular aggregation is mainly affected, the absorption spectra often displays new shifted bands, especially in the case of excimer-forming dyes[15] that feature pronounced differences when aggregation is of type H or J. We stress here that the use of the term ‘excimer’ in this context also includes ‘static excimers’, i.e., photoactive units consisting of two identical molecules associated in the ground state, with specific behavior in both absorption and emission. [16] The disappearance of bands under stress instead, may signal a more dramatic disruption of the aggregate with the transition to a full monomer-like behaviour. In fluorescence, similar reorganizations result in the quenching or enhancement of luminescence, as routinely reported again, for excimer-forming systems or as observed for solid-state luminescence enhancement (SLE) or aggregation-induced emission (AIE) chromophores[17]

where the key role in the luminescence change is likely played by the increased viscosity of the amorphous regions when under stress.

With the aim of defining a framework for a reliable atomistic description of these complex effects, in this work we present a simplified case-study focused on the simulation of a dye-polymer blend consisting in a small molecular dye embedded in a polyethylene matrix. The compound chosen is a tetraphenylethylene (TPE) derivative, see Fig.1, carrying two dimethylamino donor groups and a 3-methyl-rhodanine acceptor moiety (TPE-MRh) on three of the four TPE phenyl rings. This chromophore, that also displays SLE character, has been selected because its properties have already been investigated in a previous work[18], where the effects of different crystalline environment on TPE-MRh absorption and emission are reproduced thanks to the modeling of the environment effects on the molecules. In addition, the interest in this system also lies in the straightforward possibility to extend the study and explore the modeling of the effects of external stimuli on luminescence properties, to probe the phenomenon of *mechanofluorochromism*[19], originating from TPE-MRh aggregation-dependent emissive properties.

Harnessing the knowledge from this previous study, we have considered models composed of two possible TPE-MRh dimers as the most relevant dispersed optical units in the matrix. Since the TPE-MRh molecule features no structural symmetry, due to the grafted donor and acceptor groups to the symmetric TPE, there exist many possible dimer configurations. Here, we restrict to the two most energetically favorable structures among the possible pairs found in the lowest-energy crystal polymorph, discussed in ref. [18]. The two configurations selected from this packing differ in the reciprocal orientation of molecular axis going from the rhodanine acceptor to the *trans* dimethylamino donor. For the *parallel* dimer these molecular axes have the same orientation for the two units while for the *anti-parallel* configuration they have an opposite orientation.

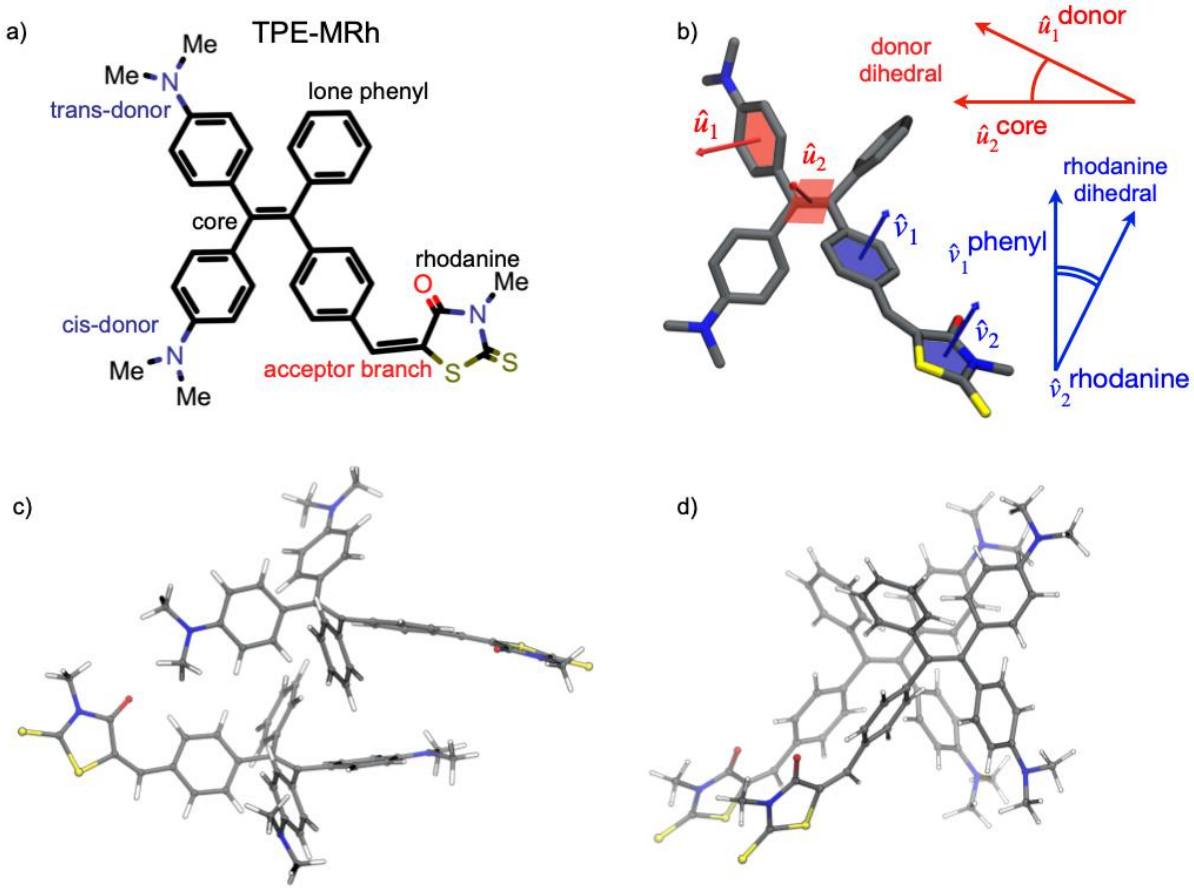

Figure 1. 2D and 3D models of TPE-MRh monomer and dimers. Panel a) TPE-MRh scheme with the moiety nomenclature used throughout the text, b) 3D model of the monomer in gas-phase geometry showing the normal vectors of the planes considered to compute the tracked structural parameters, i.e., the trans-donor dihedral (red) and the rhodanine dihedral (blue). In the bottom panels, the optimized stacking arrangements of the two dimers anti-parallel (c) and parallel (d) are shown, monomer-monomer distances are increased for clarity.

The choice of the matrix instead, has fallen on linear polyethylene due to its reduced complexity, so that even a simplified molecular model should yield an accurate enough description of the morphology in response to the stimulus and should be able to reproduce the constraining effect on the photoactive units, i.e., the TPE-MRh dimers. Indeed, the stated aim is the accurate sampling of the dimer configurations affected by the matrix constraints under stress that are then reflected in the optical response.

The manuscript is structured as it follows: after a description of the computational workflow and methods (section 2, Computational Details), in Section 3 we discuss the results concerning the photophysical properties of the isolated and embedded chromophoric units both in absence and in presence of an external mechanical stimulus up to the simulation of the macroscopic color revealing the mechanochromic behavior of the system. Finally, in Section 4, some perspectives for future improvements of the methodologies are provided.

2. Computational details

The protocol presented is based on classical molecular dynamics (MD) simulations of the sample under mechanical stress, combined with quantum chemical calculations to derive the photophysical properties of the dispersed dyes. An overall view of the workflow is reported in Fig. 2.

The simulated dye-polymer blend is composed of one optically active dimer embedded in a set of 65 polyethylene chains each composed of 20 monomeric units. The preparation of the atomistic model for the blend is the first step and is expected to provide, as an output, a realistic description of the matrix morphology around the dimers. This preparation step (Fig. 2) is articulated in two phases: 1) initialization of the box and 2) equilibration. Firstly, the simulation box is populated by the blend. The box is initially chosen to be a large cube with a side of ≈ 100 Å containing a single TPE-MRh dimer placed at the center of the box and 65 randomly disposed polymer chains. This large box allows the arrangement of all molecules while avoiding atomic overlap. During population, all structures are taken in their gas phase optimized geometry. Two different cases are considered, representing blend samples containing the *parallel* or the *anti-parallel* TPE-MRh dimer, respectively. As mentioned above, these two specific configurations have been selected since they represent the dimeric structures featured in the most stable TPE-MRh crystalline polymorph identified and studied in ref.[18].
These starting configurations are built using the Packmol package[20,21] whereas the LAMMPS[23] input files are generated with the Moltemplate tool[22].
To conclude the preparation step, these systems are equilibrated performing simulated annealing on a NPT ensemble under periodic boundary conditions (PBC) on the three cartesian directions. During this equilibration, the positions of the dimer's atoms are kept frozen at the initial geometry and the annealing is carried out exclusively on the polymer chains to obtain a representative morphology of the amorphous matrix. Heating (up to 500 K) and cooling (down to 300 K) are carried out at a rate of 25 and 20 K/ps, respectively, under constant pressure. This pressure is the one used in previous simulations of bulk polyethylene allowing us to recover the experimental density of the polymer matrix (i.e. ~0.91 g/cm^3) under the simulation conditions listed. Pressure and temperature are controlled via a Nose-Hoover chain of 5 element with relaxation times of 1 ps and 0.1 ps respectively.
All MD simulations of the matrix embedded TPE-MRh dimers are performed with the LAMMPS package[23] employing the general purpose AMBER Force Field (GAFF)[24] and a time step of 1 fs. The force field potentials and parameters employed belong to the AMBER library and, in the case of the dimer, have been selected on the basis of their ability to best fit the dimer energy profile obtained from 3 sets of single-point density functional theory (DFT) calculations where one unit is shifted with respect to the other along the stacking direction and in the two directions of the plane orthogonal to it, as detailed in Fig. S1.
Quantum chemistry calculations are then performed at the DFT level using, unless differently stated, the B3LYP functional[25–28] in combination with the 6-31G(d) basis set[29] and Grimme's D3 dispersion correction[30]. For time-dependent DFT (TD-DFT) calculations an additional set of diffuse functions has been considered, yielding the larger 6-31+G(d) basis set. All DFT calculations are carried out with the Gaussian16 software package[31].
The electrostatic charges included in the force field are obtained via restricted electrostatic potential (RESP) analysis as the AMBER protocol requires, from an Hartree-Fock calculation using the 6-31G(d) basis set on single molecule model geometries relaxed according to the aforementioned DFT level of theory.
Once an initial configuration of the blend is obtained, we proceed to the second step consisting of the blend simulation in presence of different external forces (blend simulation in Fig. 2). To this end, the system is enclosed between two rigid platelets that can mimic the external forces acting along the z-direction as the mechanical elements of a *piston*. In this setting, the simulations are carried out in a NVT ensemble where PBC along z are removed. Initially, the

chains are reconstructed along z and the two platelets are approached from sufficiently far so as to not interact with the chains. The platelets are composed of 450 dummy iron atoms each, divided in 2 layers of 15×15 atoms with an in-plane lattice spacing of 2 Å and cover the xy surface of the fundamental cell. Additional constraints are imposed to avoid their deformation and to guarantee a coherent response across the two surfaces. The system is then equilibrated to bring it back to 300 K and to a density similar to the experimental one (0.91 - 0.93 g/cm^3)[32]. This last step in particular, is necessary because the manipulations leading to the inclusion of the platelets modify the volume accessible to the blend. Indeed, while the volume of the entire simulation box is fixed during these NVT runs, the accessible volume is actually controlled by the relative position of the two platelets. Moreover, the platelets dynamic is driven by both a constant force, imposed on the system from the outside, and the internal response of the blend along z. It is found that, after the addition of the piston, the value of the experimental density is only retrieved by applying, via the platelets, an external compression of 17.4 kcal/mol·Å that is thus considered as the starting point for all subsequent simulations. In Table S1 we report the magnitudes of the forces simulated. These values roughly cover, the range between 0 and a few tens of kcal/mol·Å, in both compression and stretching. Their mapping to macroscopic values though is not straightforward since the small size of the simulated blend sample makes it difficult to relate the two quantities between the experimental and our simulated setting. For this reason, as it will be further clarified in the following we will focus on observables based on the system density. The range of densities probed thanks to the application of the forces spans values going from +30% in compression to –50% in stretching. On the same note, we have observed that, in this phase the constraint on the dimer's atoms are released. To simulate a stretching or a compression of the sample, the external force can be simply changed, but after each variation of the force, we choose to wait 300 ps in order to allow the complete decay of the transient, which, in the worst case needed ~200 ps to disappear. Only at this point the production sampling of the dimer configurations may start. Data production runs are 100 ps long and snapshots are extracted uniformly from the trajectory every 4 ps. Repeating this procedure allows the collection of configurational samples under different magnitudes of the external stimulus.

After sampling, the configurations extracted are used to build the models that will be used to predict the photophysical properties using TD-DFT methods (Optical Properties Prediction in Figure 2). Given the novelty of the protocol applied, two different approaches have been considered for the prediction of the absorption spectrum under mechanical stress. The first (MD sampling+TD-DFT, in Figure 2) considers a simple average over the set of TD-DFT computed spectra from all the sampled dimer structures extracted directly from the MD trajectories for a given magnitude of the force. The second (MD clustering QM/MM opt. + TD-DFT, in Figure 2) is based on the selection of one representative full sample structure, i.e., including polyethylene chains, for each sampling set and its use as input for a geometry optimization with a hybrid QM:MM method according to a two-layer ONIOM scheme as implemented in Gaussian16. The structure selected is the one that shows the most relevant geometrical parameters closest to the average structure computed from MD trajectories. In these latter calculations, the dimer is chosen as model systems described at high (QM) level while the rest including all polymer chains is described at low (MM) level. A constrained geometry optimization is carried out on the atoms in the high layer, while all other atoms are frozen at the positions obtained from the dynamics. The high level is the DFT model mentioned above while for low level the universal force field (UFF)[33] potentials and parameters available by

default in the Gaussian16 distribution were applied. Charges are provided matching those used during the dynamics. The geometries from these calculations are thus relaxed considering the steric hindrance and the mechanical constraints given by neighboring polymer chains and are next used as input of TD-DFT calculations for the simulation of the absorption spectra once again limited to the isolated dimer structure.
Finally, to simulate the color all vertical transitions predicted from these calculations are empirically broadened with gaussian functions with a fixed half-width at half-maximum (HWHM) of 0.3 eV. The number of transitions computed it is chosen so as to cover all relevant excitations within the range important for color, i.e., between 1.65 to 3.25 eV.

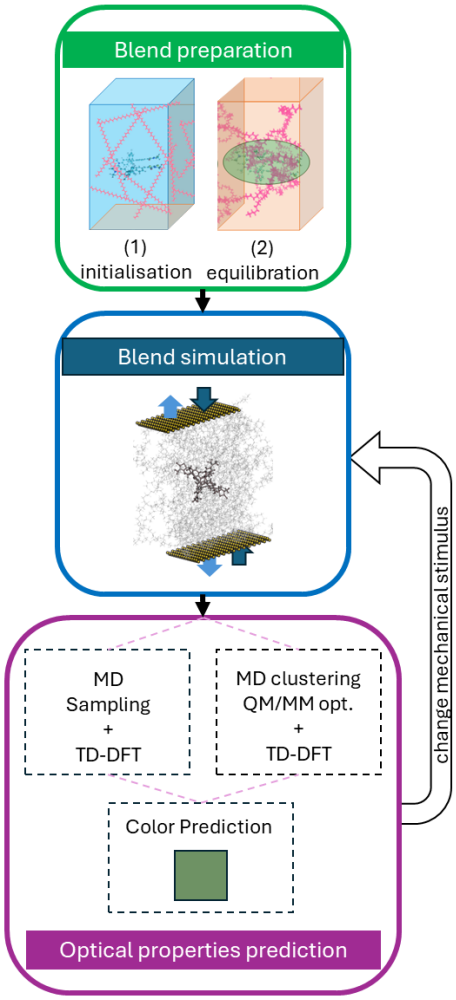

Figure 2. Schematic workflow applied to predict the optical properties of the blend as a function of an external mechanical stimulus. For details associated with the computational approaches used refer to the Computational Details.

3. Results and discussion

As amply discussed, the origin of the mechanochromic response in dye-polymer blends is ascribed to the structural modifications induced on the dyes by the polymer matrix under the external force. To analyze and decompose the different effects playing a role, we will proceed as follows. First, in Section 3.1, we will describe the gas-phase photo-physics of the isolated chromophoric units (the monomer and the dimers) and discuss the most relevant geometrical

parameters enabling their tuning to define a reference for the behavior. Next, in Section 3.2, we will consider how the structure of the dispersed chromophores (here dimers) is modified due to the external stress transmitted by the matrix reorganization around them. Finally, in Section 3.3, we will see how to simulate the impact of these structural changes induced by the matrix on absorption. In this way we will demonstrate how the proposed computational protocol enables to link the atomistic reorganization induced by the external stress to the observed absorption changes.

3.1 Photophysical properties of isolated chromophoric units.

To appreciate any change in the photo-physical properties of TPE-MRh-dispersed polyethylene, in absence or presence of external stress, the starting point is the definition of an optical system whose geometrical features and optical properties are taken as reference. The obvious choice in the context of this work, is to consider the two most stable dimer configurations, i.e., the *parallel* and *anti-parallel* ones, optimized in gas phase. Of note, in the gas phase the *parallel* dimer is predicted to be 0.88 kcal/mol more stable than the *anti-parallel* one, resulting in a ratio of roughly 80/20 for the *parallel*/*anti-parallel* at room temperature, an information that we will use further on to better assess the predictive ability of the protocol. The implied assumption that the mechanochromic behavior is mainly driven by structural modifications in the dimer and its units induced by the external solicitation[34] is supported by the fact that matrix polarization is shown to be negligible, see Fig. S7.

The absorption spectra of the two reference dimers is reported in Fig. 3 compared against the one of the monomer.

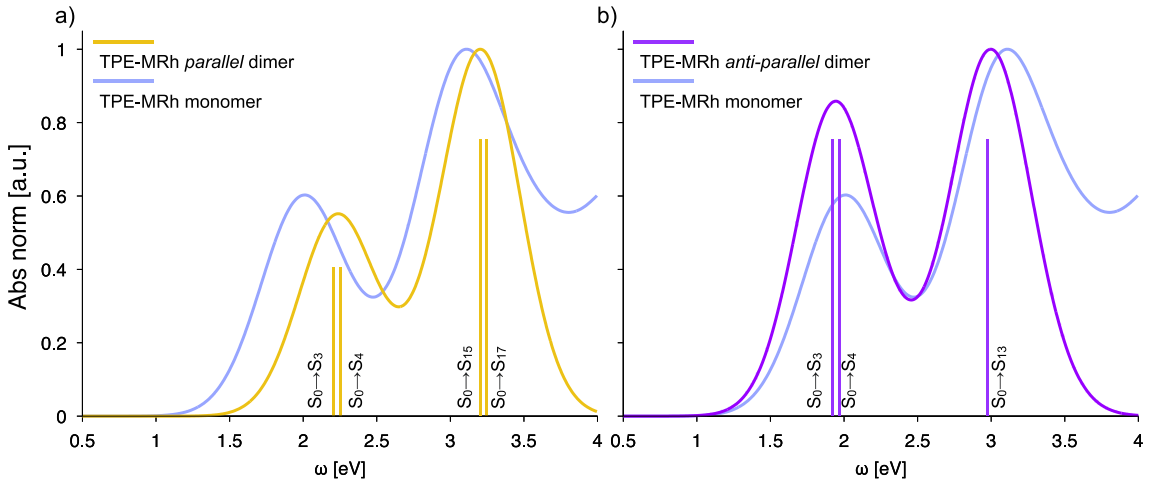

Figure 3. Normalized absorption spectra for the two dimers against the isolated monomer in gas phase. a) parallel dimer and b) anti-parallel dimer. The two structures are taken as reference for the analysis of the absorption changes induced by the polymer matrix under stress. 20 vertical transitions have been computed for all systems.

This comparison offers valuable insight into the photo-physical properties of the system. For both structures the dimerization results in the formation of excimers[35,36] featuring a dark lowest-energy excited state, that identifies them as H-aggregates according to Kasha's classification[16,37].

The analysis of the brightest states in both the monomer and the dimers allows the identification of the specific structural changes that mostly impact optical absorption. For the monomer and dimers, in the relevant range for color, i.e., 1.65 to 3.25 eV, absorption is characterized by two

bright bands. In the monomer, the first one is due to a $S_0 \rightarrow S_1$ transition that corresponds to a HOMO→LUMO transition, see Fig. S3. Here, upon excitation, electronic density increases on the acceptor branch (rhodanine moiety and phenyl) by partially depleting all the other groups attached to the central core, that act as donors. The charge transfer (CT) character has been assessed through the D_{CT} index[38] that has a magnitude of 7.5 Å (q_{CT} = 0.84 *e*) compared to a distance between rhodanine unit and trans-donor of roughly 14 Å along the main molecular axis.
The second band instead, is associated to the presence of two transitions. The dominant one, with an oscillator strength of 0.68 at 3.04 eV, features a pronounced π-π* reorganization centered on the acceptor branch and a minor charge transfer to the same moiety from the donor moieties, similar to what discussed for $S_0 \rightarrow S_1$. While the other, at 3.23 eV and corresponding to the $S_0 \rightarrow S_5$ excitation, is less bright and involves once again a partial charge transfer with a density reorganization that depletes the donors in favor, this time, of the core, the non-functionalized phenyl and the acceptor branch. The smaller CT character is confirmed by the D_{CT} values computed at 2.8 and 5.3 Å, respectively with transferred charges of 0.5 *e* for both. The natural transition orbitals associated to these transitions are reported for clarity in SI.

As already mentioned, in the case of dimers, the interactions between the different moieties of the two monomers favor the emergence of excimer behavior, that is more pronounced in the case of the parallel dimer thanks to an overall better overlap of the two structures. The parallel dimer is indeed the most stable and the estimated binding energy between its two constituent units is computed to be -38 kcal/mol. For this dimer, the brightest transitions are characterized by a density reorganization corresponding to a charge transfer from one monomer to the other. Only small structural differences between the single monomers in the dimer with respect to the isolated monomer are found (see Table S3) and, naturally, the electronic reorganizations in this structure mirror the ones seen for the single monomer, additionally involving cross charge transfers from the donor moieties of one unit to the acceptor of the other in different combinations.
The geometry of the *anti-parallel* dimer is less favorable to the coupling of the different moieties, with a computed binding energy between the monomers of -34 kcal/mol. As a consequence, the excimer character is less expressed in the set of the brightest transitions. The first band, in this case, is given by two bright transitions, $S_0 \rightarrow S_3$ and $S_0 \rightarrow S_4$. The first one involves a charge transfer from the donor moieties of both monomers to the acceptor moiety of one of the two units while the other transition is localized only on one unit and features a reorganization that is very similar to the one reported for the isolated monomer $S_0 \rightarrow S_1$ transition. This means that the low-energy band is given mainly by two transitions with CT character for which the D_{CT} is computed to at 6.8 and 5.8 Å, respectively with a transferred charge of 0.8 *e* for both.
On the other hand, the high-energy band is dominated by a single transition, $S_0 \rightarrow S_{13}$ f = 0.62, with substantial π-π* character centered on the acceptor branch of a single unit, similar to the $S_0 \rightarrow S_4$ transition observed in the monomer, with smaller contributions corresponding to : i) a CT from the donor moieties of the same unit, and ii) from the other monomer. The D_{CT} length for this excitation is 4.6 Å, while q_{CT} is 0.55 *e*.
The emergence of a more pronounced excimer character for the *parallel* dimer partially explains the difference in the relative height of the bands for the two dimers. In fact, in this system, the electronic states originating from the interaction of the two units are more complex

and result in the emergence of 2 intense transitions giving the second band, against the only one found for the *anti-parallel* dimer. These transitions have oscillator strengths of 0.62 and 0.51 and imply density reorganizations that are largely local, as they mostly concern π-π* transitions on either the donor or acceptor moieties of one of the two monomers . The presence of these peaks helps maintaining a ratio between the height of the first and second band in the parallel dimer similar to the monomer while their absence in the antiparallel case contributes to the lowering of the second band combined with geometrical effects that likely boost the brightness of the first one, as it will be clarified later.

The presence of many CT transitions involving the dimethylamino donors and the rhodanine acceptor, highlights the fact that the modulation of the coupling between these groups and the rest of the molecule has a strong effect on the absorption response. This coupling is clearly of great importance for the mechanochromic behavior that we aim to describe. While a number of structural parameters may be chosen to track how mechanochromism is elicited on the dye units by the polymer chains under stress, our analysis clearly suggests that two dihedrals specifically have the strongest impact, see Fig.S2&S3. The first one is the dihedral formed between the rhodanine ring and the phenyl in the acceptor branch, shown in Fig.1,modulating the degree of conjugation between the electron-withdrawing rhodanine ring and the rest of the structure. The second is the dihedral between the approximate plane where the double bond lies and the plane of the donor ring trans to the acceptor branch. Modifications of these two dihedrals determine often conspicuous changes in the absorption behavior for both the monomer and the dimer. In particular the modification of the rhodanine dihedral implies a considerable loss of conjugation when the group is roughly perpendicular to the phenyl. The rigid scan results available in Fig. S2 show that for values around 60˚ the second band starts losing brightness and is redshifted, with a similar effect on the first band observed for values of the angle around 90˚ while also involving a splitting. The other parameter, the trans-donor dihedral (Fig. S3), has a less pronounced effect that is mostly expressed as a modulation of the bands relative strength. With respect to what is simulated for the reference structure, the scan shows that, as the dihedral changes, the second band can grow much larger than the first or the two can show similar intensities. This modulation and the overall larger impact that the rhodanine dihedral has, are explained by the fact that one of the dominant transitions of the second band features a reorganization of the density mostly confined to the acceptor branch, that is only mildly affected by changes in the coupling between the trans-donor moiety and the rest of the structure that otherwise remain important for the dominant transition yielding the first absorption band.

Since these moieties are peripheral they are particularly sensitive to the interactions with the polymeric matrix and they will be shown to play a major role in explaining and driving the modulation in absorption observed in presence of an external stress to the structure of the dimers.

3.2 Molecular dynamics sampling under mechanical stress

The configuration samples collected from MD runs have been obtained for different magnitudes of the applied external force in both compression and stretching (see Table S1). In the following, we focus on the structures obtained for two runs simulating the stretching of the blend at different magnitudes and one run corresponding to its compression. As described in the C*omputational details* section, each sample consists of 25 snapshots extracted from the 100

ps of the production simulation, after the system has reached the equilibrium between the applied stimulus and its internal response. Given the difficulty in relating the force magnitude in the experimental and computational setting already discussed, we introduce quantities more readily comparable with observations like sample 'strain' (or 'elongation') along the direction of the force and density variation. Relative strain (s) is also commonly employed in experimental settings[39] to describe the response of polymer samples under mechanical stimuli and makes for an ideal comparative quantity. It is computed as the difference between the length of the sample along the direction of application of the force at rest and during its action. In our computational setup, this quantity is obtained by considering the distance between the piston platelets at the last frame of the simulation ($L_{\text{under stress}}$) and at the beginning, when the system represents an experimental sample in absence of external stress (L_{free}) as :

$$s = \frac{\Delta L}{L} = \frac{L_{\text{under stress}} - L_{\text{free}}}{L_{\text{free}}}$$

It is also worth recalling that, in all our simulations the direction of the external force (z-axis) is taken to be perpendicular to the molecular planes of the monomers (defined as the approximate planes containing the central double bond and the four residual bonds of the ethylene core), that are approximately parallel to each other in the dimers, see Fig.1b. Table 1 reports the values of strain in percentage on the simulated samples, together with the corresponding density variations.

Table 1. Sample strain and density variation in percentage under the different magnitudes of the mechanical stimulus simulated. The experimental reference value for polyethylene density, 0.9 g/cm^3, is also the value reached at the end of the sample preparation (Fig.2 step 2) after the inclusion of the platelets.

Blend sample	Strain	Density variation
parallel under compression	-7.1%	+8.7%
parallel under weak stretching	+5.3%	-4.4%
parallel under intense stretching	+96.9%	-48.8%
anti-parallel under compression	-8.1%	+9.2%
anti-parallel under weak stretching	+4.1%	-2.8%
anti-parallel under intense stretching	+95.7%	-49.8%

Data from Table 1 and Table S1 give a first indication of the effects of the simulated application of the force on the polymer chains. Under compression, when the dye-polymer blend in the simulation box is forced to pack more tightly, the polymer chains and the dimer experience a reduction of the available volume and hence a density increase that quickly saturates to a value of roughly 20% as the magnitude of the compression increases, as can be seen from Table S1. Under these conditions the tight packing causes the structure to have limited freedom of motion for the different peripheral groups of the dimers that are heavily constrained by the interactions with the surrounding chains. The observed structural variations involve deformations or bends of the peripheral substituents as the magnitude of the force on the sample grows.

Under stretching instead, the polymer chains are pulled apart by the action of the piston. The ones more aligned along the stimulus direction or in direct contact with the platelets are forced to straighten and unfold while others are mostly shifted, rigidly, along the z-axis without

undergoing substantial configurational changes. This process naturally results in a length increase of the system along the force direction and in the formation of empty regions in the volume associated to a lower density. The largest simulated strain amounts to roughly 100%, giving an approximate 50% density decrease for both *parallel* and *anti-parallel* samples. The formation of these empty regions inside the blend has the effect of increasing the volume available to the dyes. In these conditions, TPE-MRh dimers are then free to relax within these empty volumes inside the stretched matrix. Depending on the resulting matrix morphology, this may result in the monomers leaving apart and in the progressive loss of the interaction between the units for growing stretching magnitudes. Once again, the bulky moieties make it so that the molecules might still interact with the some of the chains and their flexibility with respect to the core results in the sampling of configurations where some of the structural parameters depart substantially from the ones of the reference structures. These changes are naturally linked to the modified optical properties.

Another general characteristics of the constraints given by the matrix under stress is that, in the dense environment of the polyethylene matrix, the dimers' conformational freedom is rather limited, especially under compression or weak stretching when the density is still sufficiently high. This changes under more intense stretching, as the formation of empty regions lets the system explore more of the conformational space while usually conserving some residual matrix constraints, e.g., stretched isolated chains in close contact with the dyes.

3.3 Optical properties under mechanical stress

After these mostly qualitative observations on the effects of the force on the matrix, the assessment of the mechanochromic behavior requires to demonstrate, as discussed, the modifications on the absorption spectra under different conditions. As mentioned, two different approaches have been compared to simulate the spectral response, (i) the average of the absorption spectra calculated for all the configurations sampled from the MD runs and (ii) the calculation of the absorption spectrum of the dimer from a representative dye-polymer configuration from the sampled set that is further optimized at QM:MM level.

To compare these two approaches, we focus on the results obtained for the *parallel* dimer only under two different stretching magnitudes, associated with elongations of 5.3% and 96.9%, respectively. The results are plotted in Fig.4.

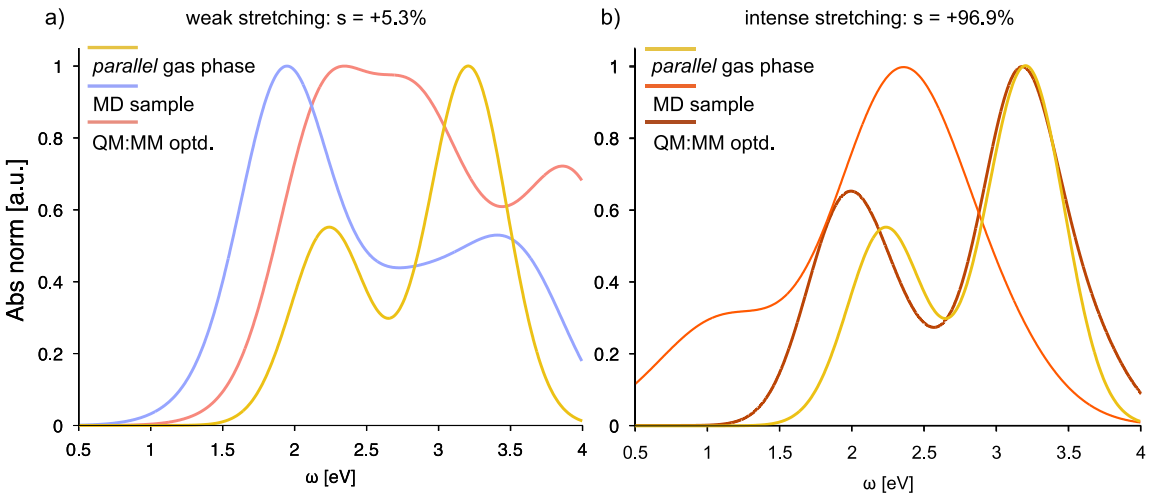

Figure 4. Comparison between TPE-MRh absorption spectra predicted from structures sampled with the blend under weak stretching *(left)* and intense stretching *(right)* according to approach (*i*) average over MD sampled dimer configurations (ii) spectrum of a representative structure from the sample optimized at QM:MM level.

The spectra simulated according to the two approaches show pronounced differences in the positions and relative intensities of the absorption peaks. These differences prompt the question of which calculation methods provides the most accurate modelling of the system. For this reason, we resort to an analysis of the behavior of the microscopic model built so far, focusing on the soundness of the classical molecular dynamics description of the most relevant identified structural degrees of freedom. We consider the QM:MM optimized structure as a plausible approximation of the equilibrium structure and we expect the structures probed by classical molecular dynamics to describe thermal oscillations around this equilibrium structure. This is plausible under the assumption that the steric constraints imposed by the surrounding polymer chains are not changing considerably along the dynamics. This assumption actually holds thanks to the fact that the polymer chains display rather rigid configurations, i.e., they express limited conformational freedom during the dynamics due to the action of the external force and the dense environment. This is clearly true under compression but also applies under weak stretching when the density is still quite high and to a lesser extent also to the case of intense stretching. In Figs. 5, 6&7 the distributions of the five dimer structural parameters along the dynamics for the system under weak and intense stretching are compared to the values of the corresponding QM:MM structures optimized from representative whose structural parameters fall, more or less, at the center of these distributions. The parameters are depicted in Fig.1b and represent i) the dihedrals of both monomers between the rhodanine ring plane and the phenyl plane in the acceptor branch (rhodanine dihedral in Fig. 5&6), ii) the dihedrals, again of both monomers, between the central bond plane and the trans-donor ring (donor dihedral in Fig. 5&6) and iii) the distance between the two monomers (computed as the distance between the double bonds' centers). The distributions computed for these structural parameters show that, for both intensity of stretching, the force field has a less-than-ideal performance when it comes to the description of the intermolecular interactions between the monomers.

This is evident in particular by inspecting Fig. 7 where the distribution of the distance between the TPE-MRh central bonds is shown to consistently miss the reference QM:MM value. The difference is more pronounced for the largest elongation probed, where the MD structures are shown to underestimate this distance of 2 Å. This rather large difference indicates that, even when the structure should have more freedom to relax, the force field is not able to recover the

equilibrium configuration. The same comparison for the dihedrals leads to somewhat similar conclusions despite an overall better performance for some of the dihedrals sampled, like the rhodanine dihedral on monomer 2 under weak stretching or the same dihedral under intense stretching. The dynamics describes a range of variation for these parameters that is sufficiently large, despite the presence of the matrix constraints, as to access conformers with pronounced shifts in the position and intensity of the absorption bands explaining the sometimes pronounced difference between the MD sampled spectrum and the one obtained from QM:MM. This unsatisfactory description provided by the force field has led us to only consider the absorption spectra obtained from the QM:MM optimized results in the following. We note that, despite the seemingly greater computational cost, the QM:MM approach has actually proven to be cheaper in the instances tested. This is due to the fact that the sampled geometries from the MD runs with the above mentioned force field, the inputs for the (LR)TD-DFT calculations, require to evaluate, for each frame, a large number of excited states (between 50 and 70) to cover the relevant energy range. More concerning from the point of view of the statistical relevance would be the reduction of the sample to a single representative structure, i.e., the relaxed one. Also for this, results on the instances tested suggest that, due to the constraining effect of the matrix under the stimulus, this is not so impactful. The actual issue is instead found to be the fixed character of the matrix morphology under stress that does not allow the exploration of a number of possible constraints put in place by the polymer around the dimers. This issue that will be addressed in further developments by considering a larger number of initial blend morphologies.

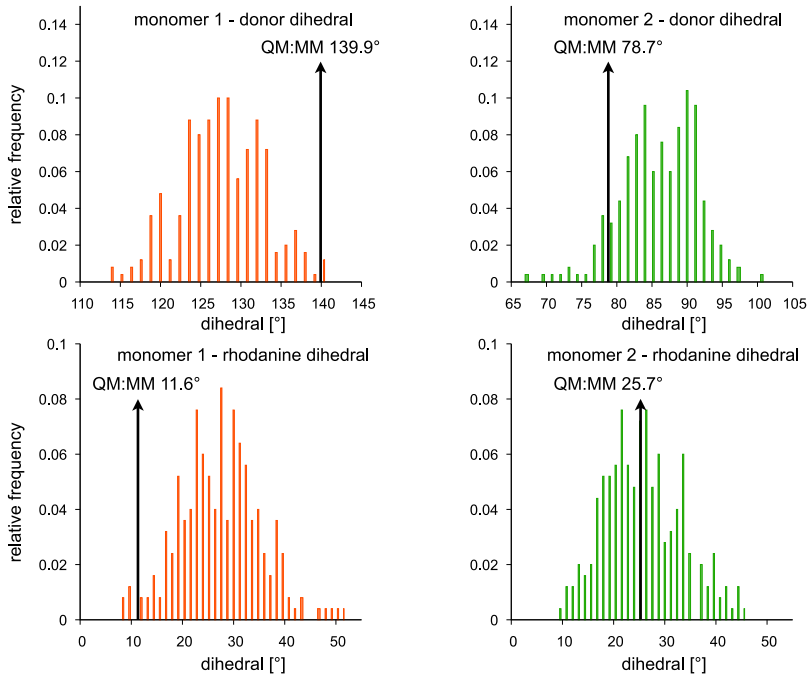

Figure 5. Histograms with the dihedrals distributions from under the +5.3% elongation simulations of the trans-donor ring with respect to the central bond plane in both units and the rhodanine ring in both units with respect to the acceptor branch phenyl, see Fig.1. The black arrows indicate the optimized values of the structural parameter from the QM:MM optimizations.

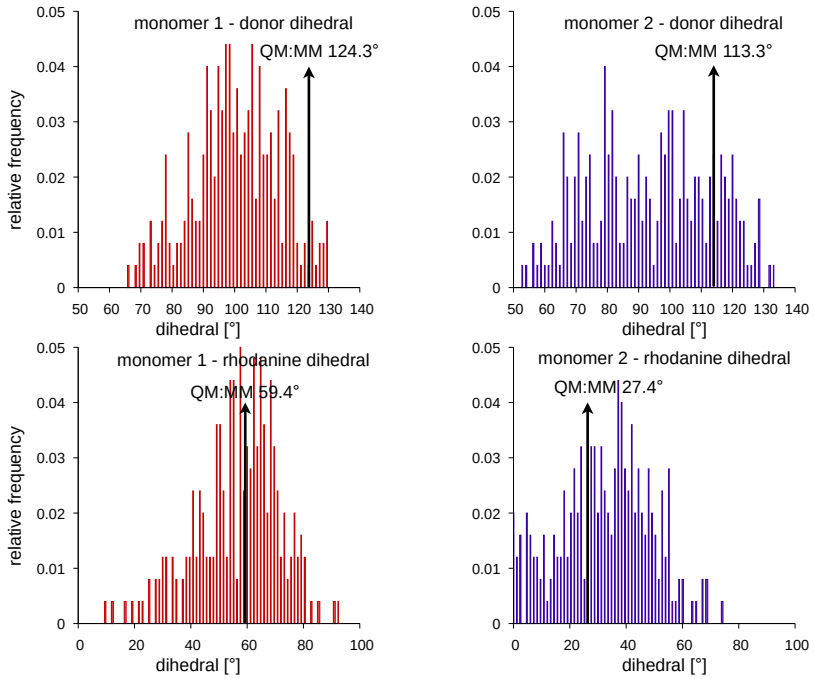

Figure 6. Histograms collecting the values of the rhodanine and trans-donor dihedrals from the MD sampling under the most intense stretching tested (elongation of 96.9%) compared with the reference values obtained via the QM:MM optimization (black arrows).

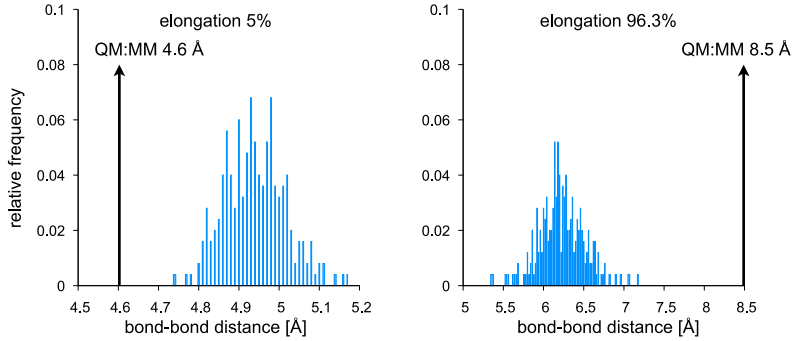

Figure 7. Histograms for the distances between the central C=C bonds of the monomers from the MD sampling under the two magnitudes of stretching considered. Black arrows indicate the values obtained from the QM:MM optimization of one representative structure extracted from the sample.

3.4 Revealing the mechanochromic behavior

We now approach the central question of how to reveal mechanochromism under the three external stimuli considered for our numerical model of the blend. As concluded above, we limit our analysis to the spectra coming from the QM:MM optimized calculations after the MD runs. The different stimuli have been considered for models hosting both the *parallel* and *anti-parallel* dimers in the matrix and include mechanical compression, giving negative elongations of -7.1% (*parallel*) and -8.7% (*anti-parallel*) along with a weak and an intense stretching, resulting in positive elongations of +5.3% (parallel) , +4.1% (*anti-parallel*) and +95.7% (*parallel*), 96.3% (*anti-parallel*), respectively.

As already remarked, the dense polymer environment, especially under compression or weak stretching, induces structural changes in the dimer packing that alter the same key structural parameters identified before, i.e., the dihedrals of the peripheral moieties. Overall, under these conditions, the packing is tighter and the respective moieties of the monomers are forced to

interact more strongly with each other within constrained molecular geometries that can be quite far from the equilibrium gas-phase ones. This is supported quantitatively by evaluating, for these structures, the average minimum distance between the atoms in the two units of the dimer. In the gas-phase *parallel* dimer this value is 3.5 Å with the smallest value in the set, i.e., *closest contact distance*, of 2.0 Å. Indeed, the interatomic distances change considerably for the matrix-dispersed system that has a smaller available volume. This can still be observed under weak stretching where the average minimum distance for the QM:MM structure, is lowered to 2.7 Å while the minimum in the set is as low as 1.5 Å, comparable with a bond distance.

The same measure for the *anti-parallel* dimer gives an average value of 3.7 Å in gas phase, in agreement with the lower dimer binding energy (-34 kcal/mol versus -38 kcal/mol). This value is decreased to 3.3 Å under weak stretching proving that the *anti-parallel* structure has a stronger repulsive interaction between the units given by the specific arrangement of the TPE-MRh monomers. It is worth noting nonetheless that, also in this case, the closest contact distance is shortened to 1.4 Å from an initial value of 2.0 Å.

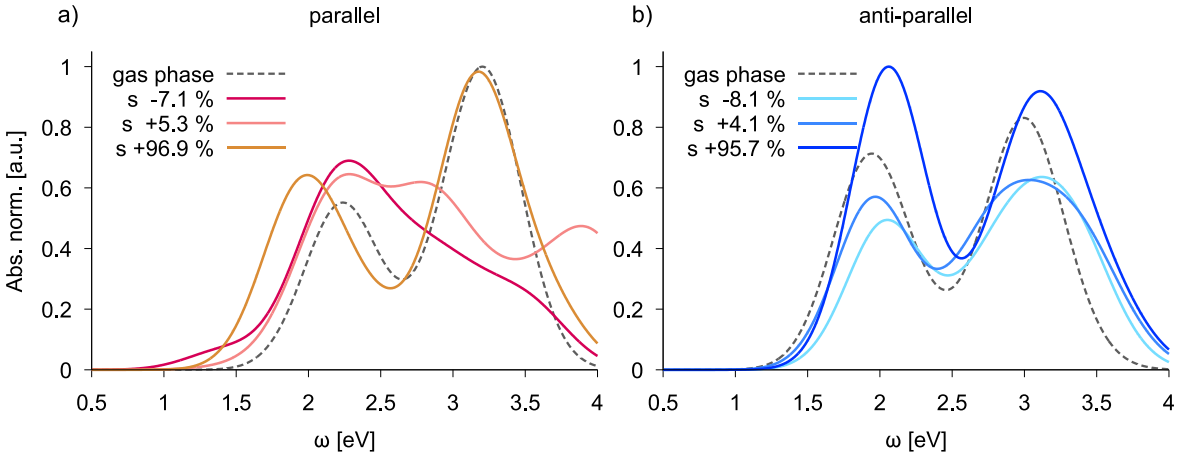

Figure 8. Absorption spectra computed for the parallel and anti-parallel dimers embedded in the polyethylene matrix under stress. Three different solicitations are considered: moderate compression, weak stretching and intense stretching, see Table S1. Spectra are normalized to the absorption value the highest peak in each set.

To assess the impact of this on the response in absorption, the spectral shape offers a straightforward comparison criterion across type and magnitude of external stimulus and between dimers. As evident from Fig. 8, the mechanical modulation of the spectrum is more pronounced for the *parallel* dimer. The modulation mostly concerns the high-energy band, that is red-shifted and lowered in intensity under compression or weak stretching before recovering, at largest elongation, a shape close to the gas-phase monomer spectrum, see Fig. 3 and Fig. S8 for direct comparison. Microscopically, this last change originates from the disruption of the dimer caused by the stretching of the matrix and strongly contributes to the marked mechanochromic effect predicted for the *parallel* dimer.

These effects on the bands can be better understood by taking a closer look at the electronic density reorganizations associated with the transitions computed under stress. Once again, we focus our discussion only on the sample under weak stretching knowing that most of the observed trends can plausibly be generalized to other conditions. In the *parallel* reference, the low-energy band (around 2.0 eV) is associated to two bright transitions implying crossed redistributions of the density between donor and acceptor moieties of both units, in different

combinations. Under weak stretching, the intermolecular interactions between the different donor and acceptor groups are more intense, due the tighter packing, yet, this denser packing comes at the cost of structural modifications concerning the dihedrals between the different aromatic units and ring planarity that translate in a partial loss of conjugation and a proliferation of states with energies in the 2.0 - 3.0 eV range and lower intensities (f between 0.1 and 0.3), associated to more local density transfers between adjacent groups, both intra and intermolecular, while featuring less often the structure-wide reorganizations described above for the reference. This is also supported by a general trend, valid for both dimer arrangements, that sees lower oscillator strengths for the systems in denser environments that give smaller absorption coefficients with the respect to the systems in less dense samples or in gas phase.
Moreover in this case, even under intense stretching the reference behavior is never recovered, as already pointed out, since stretching the matrix induces the separation of the units (distance between central bond is 8.3 Å, see Table S2) and the expression of a monomer-like response, thanks to the relaxation of the both units to a geometry close to the isolated unit within the larger free volumes.
The same analysis for the *anti-parallel* dimer explains how the different character of the packing helps maintaining an absorption response with similar characteristics across the set of external stimuli considered. Since in the *anti-parallel* stacking the excimer character is less expressed, the electronic excited states characterizing the response remain, for the most part, confined to one of the two monomers with fewer and much less substantial density reorganizations concerning moieties belonging to both units. Here, the most important consequence of the packing are the structural changes it entails that result, despite the higher density, into a further loss of the excimer character. A situation that is somewhat symmetrical to the other arrangement. Indeed, under weak stretching, the first band is still given by a very bright transition on one of the two units with CT character, while all other bright transitions contribute to the high-energy band and are characterized by density reorganizations on one of the two monomers with limited or very limited contribution from the other. A convincing proof of this is given by comparing Fig.S4&S5 in which the full dimer spectra under weak stretching are plotted against the sum of the spectra of the isolated monomers at the geometries found in the QM:MM optimized dimers. The *anti-parallel* dimer is shown to have an absorption that is very close to the sum of the absorption of the two separate units, in contrast with the result for the *parallel* dimer. Under intense stretching, also in the anti-parallel case, the distance between the two units is greatly increased (the distance between the central C=C double bonds of the two TPE-MRh units is 9.5 Å) but the spectrum remains similar to the ones reported for the other stimuli applied. Once again, this goes to show the weak interaction between the two units that maintain responses associated to the single units but also indicates the permanence of the structural modifications that determine the spectral shape under the other stimuli in more dense conditions, likely due to the constraints put in place by the polymer matrix. Modifications that are given by the initial dimer packing and are never substantially modified by the matrix under stress. Of note, under intense stretching there is also an inversion between the brightness of the first and second band.
Although our model represents a substantial simplification to the complexity of the real system, we have nonetheless attempted a comparison against the experimental data available by extrapolating our results to describe samples at larger scales (> 10 nm). To carry out this comparison we have used experimental absorption data collected for a TPE-MRh:polyethylene blend film at 1% dispersed dye in weight, see Fig. S6. Our simulated spectra have been

combined into a model (details available in the SI) and a fitting procedure has been carried out to assess the ability of our data to reproduce the observed blend spectrum.
The fit result and the experimental absorption have been used to predict the color perceived by the human eye according to an established protocol assuming specific standardized conditions ref. [40]. We have limited ourselves to the spectrum for the experimental sample at rest, i.e., under no stimulus. To build the fitting model, the simulated spectra have been combined with a set of parameters that both account for the potential errors of the methods used and allow the description of a mixture of dispersed TPE-MRh monomers and the two dimer arrangements. The relative weights of these two have been taken to be the Boltzmann weights computed from the gas-phase energy difference (82.2% for the *parallel* and 17.8% for the *anti-parallel*). The resulting plot and a comparison between the experimental output obtained and the one predicted through the fit are reported in Fig. 9. The estimated values for the parameters from the fitting procedure offer hints on the aggregation of the dispersed dyes in the blend and indications on how to refine our simulation strategy. Indeed, the results indicate that the ratio between monomers and dimers is roughly 1:1, suggesting that the mechanochromic effect associated to the dimers is strongly attenuated in real samples, as confirmed by the limited spectral variation reported under different elongations in Fig. S6. For what concerns the simulation, the DFT approach chosen, i.e., B3LYP, is shown to have a somewhat unsatisfactory performance. A substantial discrepancy of the experimental bands with respect to the computed absorption energies imposes an overall correction of +0.4 eV, larger than the established error statistics for the method[41].
While this is partly to be expected, due to the known problems of the approach, the magnitude of the discrepancy is probably amplified by an insufficient description of the molecular environment in the blend, that could improve the modeling of the structures at rest by going beyond the simple description in gas phase. Along the same line, the correction imposed on the oscillator strength of CT states, that lowers their strength of roughly 20% is introduced precisely to cure the known fallacies of a global hybrid method and converge toward a better agreement with the experimental bandshape. Overall, the color predicted is in agreement with the experimental one, hinting at the protocol potential.

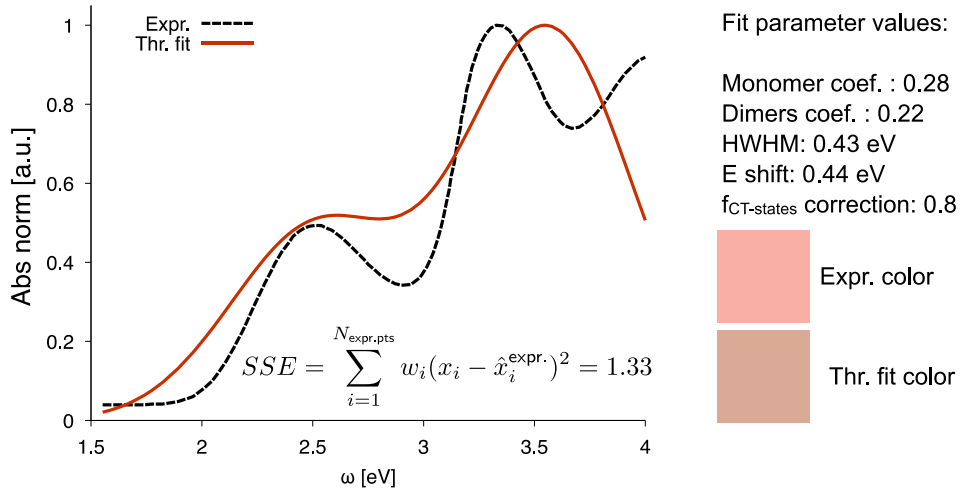

Figure 9. Normalized experimental absorption spectrum for a TPE-MRh-dispersed polyethylene blend at rest, i.e., under no solicitation, and the fit obtained by mixing the monomer and dimers spectra computed in gas phase.

Inspired by the results detailed above, we have attempted to use our simulated data to predict the perceived color of all the *in-silico* samples containing the dimers under different elongations. This has been done in order to better visualize the magnitude of the mechanochromic behavior when attempting the extrapolation to the macroscopic limit. The predicted colors, using the same protocol cited above, are available in Fig.10. To obtain all the colors shown, we have considered all the single spectra (normalized) plotted in Fig. 8 and their combination in the fixed relative Boltzmann ratio already considered before.The colors appear quite different from the ones in Fig. 9. In particular, the *parallel* dimer shows a marked change from violet, given by the excimer-enhanced absorption in the [2.0,3.0] eV range under compression or weak stretching, to a blue-green color, associated to the monomer and coming from a lowered absorption in the same range. The predictions for the *anti-parallel* dimer instead, have a much smaller variation reflecting the persistence of the spectral shape across the range of stimuli considered. A blue-green color is maintained under all different elongations and this can be directly attributed to the absorption gaps consistently featured in the spectra between 2.0 and 3.0 eV. The mixtures closely follow the trend described for the *parallel* dimer due to its predominance, suggesting that, if ideal control over the way dyes are dispersed in the polymer would be possible experimentally (i.e., if a stable blend could be designed with only dimers as dispersed dye units), the resulting material would exhibit a very apparent mechanochromic response.

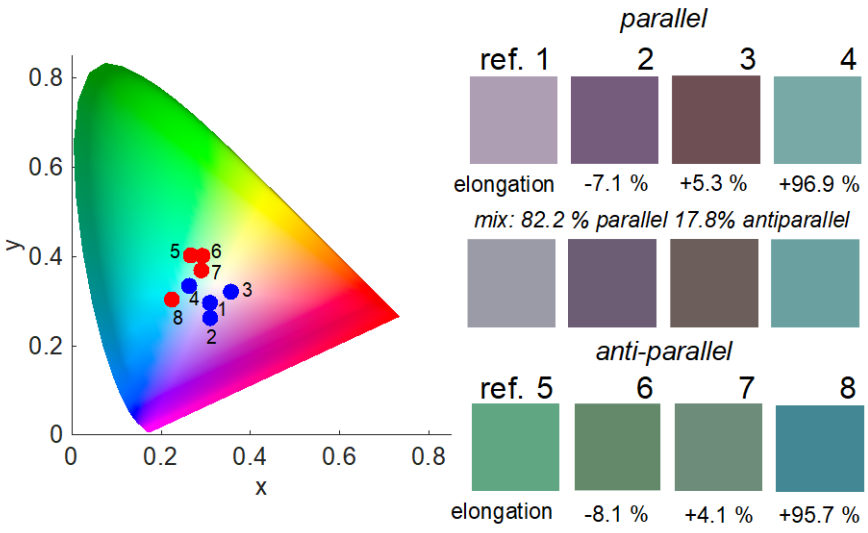

Figure 10. Color plot for the 8 systems considered. In the first row, colors predicted for the parallel dimer in gas phase (ref.1) and under different forces in compression (2) and weak (3) and intense (4) stretching. In the second row, the same results for the anti-parallel dimer in gas-phase (ref. 5) , under compression (6), weak stretching (7) and intense stretching (8). The colors shown are obtained by using the absorption spectra to calculate the transmitted spectra with respect to a standard light source and then considering the overlap with the response functions of the receptors' in the human eye, as explained in ref. 40.

4. Conclusions

In this proof-of-concept computational study we have outlined the steps of a predictive protocol for the simulation of the optical response, specifically in absorption, of a dye-polymer mechanochromic blend. We have considered a simplified atomistic model of the blend, i.e., small simulation boxes populated with short polyethylene chains hosting a single TPE-MRh dimer in two possible packing arrangements, to illustrate the procedure aiming at the simulation of physically accurate blend morphologies under external stress while preserving microscopic detail. To achieve this, a method to describe the effects of the external stress on molecular structures and packing and how they are transmitted between the components has been implemented and presented based on the inclusion of additional degrees of freedom with artificial interactions, i.e., the piston, designed to mimic the effect of the external force.

From these preliminary calculations we have been able to establish the somewhat unsatisfactory performance of the chosen force field in reproducing the molecular geometries under these non-equilibrium conditions. We have proposed a possible solution to this via QM:MM relaxations of specific configurations after the dynamics, that exploits the morphological MD data on the polymer around the chromophores to obtain representative structures of the dyes. The results have highlighted the importance of finding a way to improve the configurational sampling, mainly in terms of greatly enlarging the collected configurations statistics. This, combined with the strong dependence on the input blend morphology of the MD samplings suggests that shorter runs under stress performed on a large set of initial blend morphologies combined with QM:MM optimization on these smaller samples could provide more sound models for the molecular geometries and their responses, especially when dealing with systems as dense as the typical dye-dispersed polymer blends.

Moreover, this theoretical analysis has also been able to yield some molecular level insight on the behavior of the specific system. From the limited sampling that has been obtained, TPE-MRh mechanochromism has been found to be markedly dependent on the modulation of the excimer character of its packing and the structural parameters of the single molecules. Aspects that are both heavily influenced by the matrix, especially when aggregates as small as the noncovalent dimers are concerned. Lastly, the fit procedure has highlighted that to achieve an accurate modeling of the mechanochromic effect at larger scales, the character of the aggregation of the dispersed dyes and its thermodynamics, e.g., tendency to diffuse and disperse, thanks to a good solubility in the polymer or to diffuse and aggregate, is a key parameter in the mechanochromic character of a blend, suggesting that different experimental techniques for production may yield samples with very different performances.

Acknowledgments

This work was granted access to the HPC resources of IDRIS under the allocation 20*23*-A0150810135 made by GENCI. Dr Cosimo Micheletti is acknowledge for the synthesis of the dye. Q.W. acknowledges funding from the China Scholarship Council (CSC). C.A. acknowledge funding by the European Union (ERC AdG, project MaMa, n. 101097351). Views and opinions expressed are however those of the author(s) only and do not necessarily reflect those of the European Union or the European Research Council Executive Agency. Neither the European Union nor the granting authority can be held responsible for them.

References

(1) Fisher DJ (2019) Mechanochromism. Materials Research Forum LLC.

(2) Traeger H, Kiebala DJ, Weder C, Schrettl S (2021) From Molecules to Polymers—Harnessing Inter- and Intramolecular Interactions to Create Mechanochromic Materials. Macromol. Rapid Commun. 42 (1): 2000573. https://doi.org/10.1002/marc.202000573.

(3) Deneke N, Rencheck ML, Davis CS (2020) An Engineer's Introduction to Mechanophores. Soft Matter 16 (27): 6230–6252. https://doi.org/10.1039/D0SM00465K.

(4) Boulatov, R. (2015) Polymer Mechanochemistry. Topics in Current Chemistry 369. https://doi.org/10.1007/978-3-319-22825-9.

(5) Caruso MM, Davis DA, Shen Q, Odom SA, Sottos NR, White SR, Moore JS (2009) Mechanically-Induced Chemical Changes in Polymeric Materials. Chem. Rev. **2** 109 (11): 5755–5798. https://doi.org/10.1021/cr9001353.

(6) Patrick JF, Robb MJ, Sottos NR, Moore JS, White SR (2016) Polymers with Autonomous Life-Cycle Control. Nature 540 (7633): 363–370. https://doi.org/10.1038/nature21002.

(7) Geckeler KE, Nishide H (2009) Advanced Nanomaterials, Wiley. https://doi.org/10.1002/9783527628940.

(8) Deneke N, Rencheck ML, Davis CS (2020) An Engineer's Introduction to Mechanophores. Soft Matter 16 (27): 6230− 6252.

(9) Tabatabaeian A, Liu S, Harrison P, Schlangen E, Fotouhi MA (2022) Review on Self-Reporting Mechanochromic Composites: An Emerging Technology for Structural Health Monitoring. Compos. Part A Appl. Sci. Manuf. 163: 107236.

(10) Traeger H, Kiebala D, Calvino C, Sagara Y, Schrettl S, Weder C, Clough JM (2023) Microscopic Strain Mapping in Polymers Equipped with Non-Covalent Mechanochromic Motifs. Mater. Horizons 10 (9): 3467−3475.

(11) Brütting W, Berleb S, Egerer G, Schwoerer M, Wehrmann R, Elschner A (1997) Full Colour Electroluminescence Using Dye-Dispersed Polymer Blends. Synth. Met. 91 (1–3): 325–327. https://doi.org/10.1016/S0379-6779(98)80050-7.

(12) Kobayashi Y, Okajima S, Fukuda K (1971) Preferential Absorption of Dye to the Higher Order Amorphous Region. Seni Gakkaishi 27 (3): 102–107. https://doi.org/10.2115/fiber.27.102.

(13) Pucci A, Ruggeri G (2011) Mechanochromic Polymer Blends. J. Mater. Chem. 21 (23): 8282. https://doi.org/10.1039/c0jm03653f.

(14) Yamakado T, Saito S (2022) Ratiometric Flapping Force Probe That Works in Polymer Gels. J. Am. Chem. Soc. 144 (6): 2804–2815. https://doi.org/10.1021/jacs.1c12955.

(15) Kasha M, Rawls HR, El-Bayoumi MA (1965) The exciton model in molecular spectroscopy. Pure Appl. Chem. 11 (3–4): 371–392. https://doi.org/10.1351/pac196511030371

(16) Winnik, F. M. (1993). Photophysics of preassociated pyrenes in aqueous polymer solutions and in other organized media. Chem. Rev 93 (2), 587-614. https://doi.org/10.1021/cr00018a001

(17) Pucci A (2019) Mechanochromic Fluorescent Polymers with Aggre gation-Induced Emission Features. Sensors 19 (22): 4969. https://doi.org/10.3390/s19224969.

(18) Micheletti C, Wang Q, Ventura F, Turelli M, Ciofini I, Adamo C, Pucci A (2022) Red-Emitting Tetraphenylethylene Derivative with Aggregation-Induced Enhanced Emission for Luminescent Solar Concentrators: A Combined Experimental and Density Functional Theory Study. Aggregate 3 (2): e188. https://doi.org/10.1002/agt2.188.

(19) Xu J, Chi Z (2014) Mechanochromic Fluorescent Materials: Phenomena, Materials and Applications Royal Society of Chemstry, London https://doi.org/10.1039/9781782623229-00001.
(20) Martínez JM, Martínez L (2023) Packing Optimization for Automated Generation of Complex System's Initial Configurations for Molecular Dynamics and Docking. J. Comput. Chem. 24 (7): 819–825. https://doi.org/10.1002/jcc.10216.
(21) Martínez L, Andrade R, Birgin EG, Martínez JM (2009) PACKMOL: A package for building initial configurations for molecular dynamics simulations. J. Comput. Chem. 30 (13): 2157–2164. https://doi.org/10.1002/jcc.21224.
(22) Jewett AI, Stelter D, Lambert J, Saladi SM, Roscioni OM, Ricci M, Autin L, Maritan M, Bashusqeh SM, Keyes T, Dame RT, Shea JE, Jensen GJ, Goodsell DS (2021) Moltemplate: A Tool for Coarse-Grained Modeling of Complex Biological Matter and Soft Condensed Matter Physics. J. Mol. Biol. 433 (11): 166841. https://doi.org/10.1016/j.jmb.2021.166841.
(23) Thompson AP, Aktulga HM, Berger R, Bolintineanu DS, Brown WM, Crozier PS, in 't Veld PJ, Kohlmeyer A, Moore SG, Nguyen TD, Shan R, Stevens MJ, Tranchida J, Trott C, Plimpton SJ (2022) LAMMPS - a Flexible Simulation Tool for Particle-Based Materials Modeling at the Atomic, Meso, and Continuum Scales. Comput. Phys. Commun. 271: 108171. https://doi.org/10.1016/j.cpc.2021.108171.
(24) Wang J, Wolf RM, Caldwell JW, Kollman PA, Case DA (2004) Development and Testing of a General Amber Force Field. J. Comput. Chem. 25 (9): 1157–1174. https://doi.org/10.1002/jcc.20035.
(25) Vosko SH, Wilk L, Nusair M. (1980) Accurate Spin-Dependent Electron Liquid Correlation Energies for Local Spin Density Calculations: A Critical Analysis. Can. J. Phys. 58 (8): 1200–1211. https://doi.org/10.1139/p80-159.
(26) Becke AD (1992) Density-functional Thermochemistry. I. The Effect of the Exchange-only Gradient Correction. J. Chem. Phys. 96 (3): 2155–2160. https://doi.org/10.1063/1.462066.
(27) Lee C, Yang W, Parr RG (1988) Development of the Colle-Salvetti Correlation-Energy Formula into a Functional of the Electron Density. Phys. Rev. B 37 (2): 785–789. https://doi.org/10.1103/PhysRevB.37.785.
(28) Stephens PJ, Devlin FJ, Chabalowski CF, Frisch M (1994) J. Ab Initio Calculation of Vibrational Absorption and Circular Dichroism Spectra Using Density Functional Force Fields. J. Phys. Chem. 98 (45): 11623–11627. https://doi.org/10.1021/j100096a001.
(29) Rassolov VA, Ratner MA, Pople JA, Redfern PC, Curtiss LA (2001) 6-31G* Basis Set for Third-Row Atoms. J. Comput. Chem.22 (9): 976–984. https://doi.org/10.1002/jcc.1058.
(30) Grimme S. (2011) Density Functional Theory with London Dispersion Corrections. WIREs Comput. Mol. Sci. 1 (2): 211–228. https://doi.org/10.1002/wcms.30.
(31) Frisch MJ et al. (2016) Gaussian 16 Rev. C.01
(32) Haynes WM. (2016) CRC Handbook of Chemistry and Physics, 97th ed. CRC Press: Boca Raton. https://doi.org/10.1201/9781315380476.
(33) Casewit CJ, Colwell KS, Rappe AK (1992) Application of a Universal Force Field to Organic Molecules. J. Am. Chem. Soc. 114 (25): 10035–10046. https://doi.org/10.1021/ja00051a041.
(34) Calvino C, Neumann L, Weder C, Schrettl S (2017) Approaches to Polymeric Mechanochromic Materials. J. Polym. Sci. Part Polym. Chem. 55 (4): 640–652. https://doi.org/10.1002/pola.28445.
(35) Jenekhe SA, Osaheni JA (1994) Excimers and Exciplexes of Conjugated Polymers. Science 265 (5173): 765–768. https://doi.org/10.1126/science.265.5173.765.
(36) Löwe C, Weder C (2002) Oligo(p-Phenylene Vinylene) Excimers as Molecular Probes: Deformation-Induced Color Changes in Photoluminescent Polymer Blends. Adv. Mater. 14 (22): 1625–1629.

(37) McRae EG, Kasha M (1958) Enhancement of Phosphorescence Ability upon Aggregation of Dye Molecules. J. Chem. Phys. 28 (4): 721–722. https://doi.org/10.1063/1.1744225.
(38) Le Bahers T, Adamo C, Ciofini I (2011) A Qualitative Index of Spatial Extent in Charge-Transfer Excitations. J. Chem. Theory Comput. 7 (8): 2498–2506. https://doi.org/10.1021/ct200308m.
(39) Gedde U, Hedenqvist MS (2019) Fundamental Polymer Science.Springer Cham. Springer. https://doi.org/10.1007/978-3-030-29794-7
(40) Jacquemin D, Brémond E, Ciofini I, Adamo C (2012) Impact of Vibronic Couplings on Perceived Colors: Two Anthraquinones as a Working Example. J. Phys. Chem. Lett. 3 (4): 468–471. https://doi.org/10.1021/jz201552x.
(41) Tirado-Rives J, Jorgensen WL (2008) Performance of B3LYP Density Functional Methods for a Large Set of Organic Molecules. J. Chem. Theory Comput. 4 (2): 297–306. https://doi.org/10.1021/ct700248k.